

The scaling region of the lattice $O(N)$ sigma model at finite temperature

Costas G. Strouthos^a and Ioannis N. Tziligakis^b

^a *Department of Physics, University of Wales Swansea,
Singleton Park, Swansea SA2 8PP, U.K.*

^b *Department of Physics, University of Illinois at Urbana-Champaign,
Urbana, Illinois 61801-3080, U.S.A.*

ABSTRACT: We present results from numerical studies of the finite temperature phase transition of the $(3+1)d$ $O(N)$ -symmetric non-linear sigma model for $N = 1, 2$ and 3 . We study the dependence of the width of the $3d$ critical region on N and we show that the broken phase scaling region is much wider for $N = 2$ and 3 than for $N = 1$. We also compare the widths of the critical region in the low T and high T phases of the $O(2)$ model and we show that the scaling region in the broken phase is much wider than in the symmetric phase. We also report results for the width of the scaling regions in the low T phase $(2+1)d$ Ising model and we show that the spatial correlation length has to be approximately twice the lattice temporal extent before the $2d$ scaling region is reached.

KEYWORDS: Lattice Quantum Field Theory, Sigma Models, Thermal Field Theory.

1. Introduction

The behavior of symmetries at finite temperature is one of the most outstanding and relevant problems in current areas of particle physics such as cosmology, relativistic heavy-ion collisions and the quark-gluon plasma. It was shown some time ago that spontaneously broken symmetries in quantum field theories get restored at sufficiently high temperature [1]. In the high temperature limit, however, perturbation theory becomes unreliable when infrared divergences are not properly summed. Various groups developed temperature dependent renormalization group techniques to study the critical properties of the $O(N)$ scalar field theories (for a few examples see [2] and references therein).

In recent years considerable work has been done on the physics of the finite temperature chiral phase transition in QCD and related models. A compelling idea based on universality and dimensional reduction first put forward in [3], is that in QCD with two massless quarks the physics near the transition can be described by the three-dimensional $O(4)$ -symmetric sigma model. Although, there is little disagreement that the chiral phase transition in QCD is second order, no quantitative work or simulations have been done that decisively determine its universality class, because simulations are performed away from the continuum limit on small volumes and show substantial discretization and finite size effects. The knowledge of the scaling relations are crucial for a successful extrapolation to small mass and large volume near T_c .

The reasoning behind the dimensional reduction scenario is based on the dominance of the light degrees of freedom near T_c . In the imaginary time formalism of finite temperature field theory a given system is defined on a manifold $S^1 \times R^d$ with the inverse temperature $\beta \equiv T^{-1}$ being the circumference of S^1 . The boundary condition in the time direction is periodic for bosons and anti-periodic for fermions. At temperatures larger than the physical scales of the system, the nonzero Matsubara modes acquire a heavy mass and non-static configurations are strongly suppressed in the Boltzmann sum. If the original four-dimensional theory has fermions, then because of the anti-periodicity in the temporal direction, all fermionic modes become massive and can be integrated over. This is not to say that non-static modes have no effect. Rather they generate counter-terms to the three-dimensional theory. The physical picture of the dimensional reduction scenario can be described nicely by using a slightly different language presented in [4]. As one approaches the critical point, the fluctuations in space become correlated over a distance ξ which diverges at the critical point. In the critical region, not only do the fluctuations extend over large spatial scales, they also become very slow and there is a divergent relaxation time τ ; the effect is known as critical slowing down. The appropriate quantum of energy is then $\hbar\omega_c$ with $\omega_c \sim 1/\tau$. Hence if the

transition is at a finite temperature T_c , $\hbar\omega_c \ll k_B T$ near the critical point, which means that long wavelength fluctuations are classical thermal fluctuations and quantum mechanics is irrelevant. Equivalently, since the time interval β is very short compared to the relaxation time τ , typical time histories will consist of a single configuration which is the same at each time slice. The dynamics therefore drops out of the problem and a Boltzmann weight $\exp(-\beta H_{\text{classical}})$ is recovered from the path integral.

In this work we study numerically the finite temperature transition both in the $(3+1)d$ and $(2+1)d$ ϕ^4 model. This is equivalent to studying the phenomenon of dimensional crossover in a d -dimensional layer $O(N)$ spin model of infinite extent in $d-1$ dimensions and finite thickness in the remaining dimension. In other words temperature effects become predominant as a consequence of a change in dimension. The formal derivations of the dimensional reduction scenario require that the scalar mass is small compared to the temperature. We check whether this condition is necessary and we study the effects of the infrared fluctuations on the width of the critical region under different circumstances. We performed simulations of the model with different $O(N)$ (for $N = 1, 2$ and 3) symmetries in $(3+1)d$ and study the dependence of the width of the $3d$ scaling region on N . In the case of the $(3+1)d$ $O(2)$ model we compare the widths of the scaling region in the low temperature broken phase and the high temperature symmetric phase. We also study the scaling region of the $(2+1)d$ $O(1) \equiv Z_2$ model. In addition we are interested to see how finite size effects can distort the results in such a simple model that can be simulated on lattices with relatively large temporal and spatial sizes. We extract critical exponents by measuring the order parameter, the susceptibility, and the correlation length.

2. The model

In the continuum limit the Lagrangian of the model reads:

$$\mathcal{L} = \frac{1}{2}(\partial\vec{\phi})^2 + \frac{m_0^2}{2}\vec{\phi}^2 + \frac{g}{4!}(\vec{\phi}^2)^2. \quad (2.1)$$

In order to study the problem of symmetry restoration in a non-perturbative way, we regard this model as an effective low energy theory by introducing a lattice regularization with a lattice constant $a = 1/\Lambda$, where Λ is the ultraviolet cut-off. Summing the bare Lagrangian over all lattice sites and transforming the continuum parameters into suitably defined lattice parameters according to a standard convention

$$a\vec{\phi}(x) = \kappa^{1/2}\vec{\Phi}_x, \quad a^2 m_0^2 = \frac{2-4\lambda}{\kappa} - 8, \quad g = \frac{24\lambda}{\kappa^2}, \quad (2.2)$$

we are led to the following action:

$$S[\vec{\Phi}] = \sum_x \left[-\kappa \sum_{\mu} \Phi_x^{\alpha} \Phi_{x+\mu}^{\alpha} + \Phi_x^{\alpha} \Phi_x^{\alpha} + \lambda (\Phi_x^{\alpha} \Phi_x^{\alpha} - 1)^2 \right], \quad (2.3)$$

where the index μ runs over the nearest neighbors, ($\mu = 1, \dots, d$), and the index α runs over the N components of the field $\vec{\Phi}$. For convenience, in our numerical work we concentrated on the limit of an infinitely strong bare coupling where the field $\vec{\Phi}$ is constrained to unit length: $\vec{\Phi} \cdot \vec{\Phi} = 1$. In this case the action S reduces to the form:

$$S[\Phi] = -\kappa \sum_{x,\mu} \Phi_x^{\alpha} \Phi_{x+\mu}^{\alpha}, \quad (2.4)$$

which is equivalent to the energy of a configuration of the classical ferromagnetic $O(N)$ spin model.

Finite physical temperature on the lattice means a finite size of the temporal extent L_t . The physical temperature is given by $T = 1/(L_t a)$. The temperature of the system may be altered, by varying either the coupling κ , which amounts to varying the lattice spacing or by varying L_t . To minimize the effects of lattice artifacts the condition $\Lambda \gg T$ must be satisfied which requires a lattice temporal extent $L_t \gg 1$. This condition not being met implies that the sum over the Matsubara modes is truncated at a small value. It is well-known that the $(3+1)d$ renormalized ϕ^4 theory is a free theory. However, the regularized theory may well describe the correct physics of a broad spectrum of processes below the cut-off scale.

As discussed in [5] the regularized model can be interpreted in terms of physical terms by moving along the curves of constant physics (CCPs) which are characterized by $g_R = \text{const}$. Therefore, when approaching the $T = 0$ second order critical line the mass of the sigma meson M_{σ} decreases and in order to keep T/M_{σ} constant one has to increase L_t . Near the $T = 0$ critical line the ratio T/M_{σ} should not change any more along a CCP. It was shown within a specific regularization scheme to leading order in $1/N$ [6] that $T_c/M_{\sigma} = \sqrt{36/(Ng_R)}$ and by solving the gap equation on the lattice it was shown [5] that the corrections due to a finite L_t are negligible for $L_t \geq 4$. In order to suppress possible discretization effects arising from $1/N$ corrections we performed our simulations with $L_t = 12$. The $(2+1)d$ ϕ^4 theory has an interacting continuum limit and it has been shown that the non-linear sigma model is renormalizable in the $1/N$ expansion [7]. The phenomenon of symmetry restoration at finite temperature in the three-dimensional theory was investigated by means of lattice simulations and finite size scaling techniques by Bimonte et al. [8]. The authors of [8] located the intersections of critical lines corresponding to different values of L_t with various CCPs lying in the ordered phase of the $T = 0$ theory and showed that for $L_t \geq 3$ the critical temperatures approach the finite physical temperature of the continuum theory.

Furthermore, the condition $L_s \gg \xi$ must be satisfied in order to obtain results that approximate the thermodynamic limit. For this reason at certain values of coupling κ we performed simulations on lattices with different spatial extent in order to detect and control finite size effects.

In our simulations we used the single-cluster algorithm [9], because it reduces dramatically the correlations between successive configurations near a critical point. The cluster update is as follows: First choose randomly a reflection axis in the plane, denote the component of the spin $\vec{\Phi}_i$ that is parallel to this reflection axis by Φ_i^{\parallel} and that which is orthogonal by Φ_i^{\perp} . Then choose randomly a site i of the lattice as a starting point for the cluster \mathcal{C} . Visit all neighbor sites j of i and allow them to join the cluster with probability

$$p(i, j) = 1 - \exp[-\kappa(\Phi_i^{\perp}\Phi_j^{\perp} + |\Phi_i^{\perp}\Phi_j^{\perp}|)]. \quad (2.5)$$

After this is done, visit all neighbors of the new sites in the cluster and add them to the cluster with probability $p(i, j)$. Iterate this step until no new sites enter the cluster. Finally flip the signs of all Φ_i^{\perp} contained in the cluster.

3. The observables

In this section we present the various observables measured in the broken and symmetric phases of the model in our lattice simulations. The magnetization M^α of a given configuration is defined as:

$$M^\alpha \equiv \frac{1}{V} \sum_x \Phi_x^\alpha, \quad (3.1)$$

where $V \equiv L_s^3 L_t$ is the space-time volume. However, in a finite volume and without the benefit of an explicit symmetry breaking interaction with an external magnetic field, the direction of symmetry breaking changes over the course of the run so that M^α averages to zero over the ensemble. It is in this way that the absence of spontaneous symmetry breaking on a finite lattice is enforced. Another option is to introduce a field operator

$$\Phi_{\sigma,x} \equiv \frac{\Phi_x^\alpha M^\alpha}{|M|}, \quad (3.2)$$

which is a projection of Φ_x^α to the direction of M^α separately for each configuration [10]. The effective order parameter

$$\Sigma \equiv \frac{1}{V} \langle \sum_x \Phi_{\sigma,x} \rangle = \langle |M| \rangle, \quad (3.3)$$

differs from the true order parameter extrapolated to the zero magnetic field limit by a factor $V^{-\frac{1}{2}}$ [11]. One can easily show that the susceptibility of the order parameter can be expressed in terms of moments of the magnetization as follows:

$$\chi = V(\langle |M|^2 \rangle - \langle |M| \rangle^2). \quad (3.4)$$

In the symmetric phase one gets $\chi = V\langle |M|^2 \rangle$. Cluster algorithms enable us to reduce the variance of the expectation values in the symmetric phase by using improved estimators [9, 12]. The improved estimator for the susceptibility is given by:

$$\chi_{\text{imp}} = \left\langle \frac{N}{|C|} \left(\sum_{i \in C} \Phi_i^\perp \right)^2 \right\rangle, \quad (3.5)$$

where $|C|$ denotes the number of spins in the cluster C .

We determined the temporal exponential correlation length ξ_{exp}^t of the sigma meson from the asymptotic exponential decay of the zero momentum connected two-point correlation function constructed from the field $\Phi_{\sigma,x}$, i.e.,

$$O(t) = \sum_{\vec{x}} \Phi_{\sigma,x} \quad (3.6)$$

$$G(t) \equiv \langle O_0 O_t \rangle - \Sigma^2 \stackrel{t \gg 1}{\approx} A \left[\exp\left(\frac{-t}{\xi_{\text{exp}}}\right) + \exp\left(\frac{-(L_t - 1)}{\xi_{\text{exp}}}\right) \right]. \quad (3.7)$$

Similarly, we measured the spatial correlation length ξ_{exp}^s from the exponential decay of $G(x)$ in the spatial direction. The asymmetry of the lattice at nonzero temperature implies that $\xi_{\text{exp}}^s \neq \xi_{\text{exp}}^t$, because temperature effects on the mesonic self-energy become direction dependent. The breaking of Lorentz invariance implies that the spectral functions and the dispersion relations are modified in a non-trivial way by the thermal statistical ensemble. However, both ξ_{exp}^s and ξ_{exp}^t are expected to diverge as $T \rightarrow T_c$ according to the scaling law $\sim (T_c - T)^{-\nu}$, where ν is a critical exponent of the corresponding $O(N)$ $3d$ spin model. One can construct correlation functions from various other operators $O(t)$ that couple to the scalar particle σ , but according to [10] the operators we defined in eq.(3.6) give a better signal than other options. In the symmetric phase the two-point correlation function is $G(t) = \left\langle (\sum_i \vec{\Phi}(\vec{x}_i, t)) \cdot \sum_j (\vec{\Phi}(\vec{x}_j, 0)) \right\rangle$ and its improved estimator is given by

$$G(t)_{\text{imp}} = \left\langle \frac{N}{|C|} \delta_{ij}(\mathcal{C}) \Phi_i^\perp \Phi_j^\perp \right\rangle, \quad (3.8)$$

where $\delta_{ij}(\mathcal{C}) = 1$ if i and j belong to the same cluster otherwise $\delta_{ij}(\mathcal{C}) = 0$ [9, 12].

We also measured the so-called second moment correlation length $\xi_{2\text{nd}}$, defined by

$$\xi_{2\text{nd}}^2 \equiv \frac{1}{2d} \frac{\sum_x |x|^2 G(x)}{\sum_x G(x)} = - \left(\bar{G}^{-1}(k^2) \frac{d}{dk^2} \bar{G}(k^2) \right)_{k^2=0}, \quad (3.9)$$

where $\bar{G}(k) \equiv \sum_j \langle \exp(ikx_j) \vec{\Phi}_0 \vec{\Phi}_j \rangle$ is the Fourier transform of the two-point correlation function. On the lattice $\xi_{2\text{nd}}$ is expressed as

$$\xi_{2\text{nd}} = \left(\frac{(\chi/F) - 1}{4 \sin^2(\pi/L)} \right)^{1/2}, \quad (3.10)$$

where $L = L_t$ or L_s , $F \equiv \bar{G}(k)|_{|k|=2\pi/L}$. The improved $\xi_{2\text{nd}}$ requires $\bar{G}(k)_{\text{imp}}$ given by

$$\bar{G}(k)_{\text{imp}} = \left\langle \frac{N}{|\mathcal{C}|} \left[\left(\sum_{i \in \mathcal{C}} \Phi_i^\perp \cos(kx_i) \right)^2 + \left(\sum_{i \in \mathcal{C}} \Phi_i^\perp \sin(kx_i) \right)^2 \right] \right\rangle. \quad (3.11)$$

This estimator of the correlation length is very popular, because its numerical evaluation is simpler than that of the exponential correlation length which requires an identification of an asymptotic exponential decay. However, the two definitions of the correlation length do not coincide, since in ξ_{exp} only the ground state enters, while in the case of $\xi_{2\text{nd}}$ according to eq.(3.9) a mixture of the full spectrum is taken into account. As mentioned in [13] the difference from one of the ratio $\xi_{\text{exp}}/\xi_{2\text{nd}}$ gives an idea of the density of the lowest states of the spectrum. It is well-known however, that in the high temperature phase the asymptotic exponential decay behavior of $G(t)$ is reached at much smaller values of t than in the broken phase (see e.g. [13]). This behavior of $G(t)$ implies that the difference between ξ_{exp} and $\xi_{2\text{nd}}$ in the symmetric phase is smaller than in the broken phase. In our simulations we measured $\xi_{2\text{nd}}$ only in the symmetric phase and we observed that the difference between ξ_{exp} and $\xi_{2\text{nd}}$ vanishes within error.

4. Results

In this section we present results from numerical simulations of the four-dimensional $O(N)$ ($N = 1, 2$ and 3) non-linear sigma model at $T \neq 0$. We also present results from simulations performed in the low temperature phase of the three-dimensional Ising model. By measuring the correlation length ξ at the crossover into the $3d$ scaling region we study the dependence of the width of the critical region on the symmetry group $O(N)$ and on whether the symmetry is manifest ($T > T_c$) or broken ($T < T_c$). We define the crossover coupling κ_{cross} as the value of κ that if it is included in the fitting window, the extracted exponent β_{mag} does not

agree within statistical error with the exponent of the $3d$ model β_{mag}^{3d} . As we show in the next paragraphs, the change in the value of the exponent is accompanied by a substantial increase in the $\chi^2/\text{d.o.f.}$ of the fit, implying that the quality of the fit drops rapidly once we enter the crossover region. We managed to identify the value of κ_{cross} with relatively good accuracy, because as we will see in the following paragraphs the value of κ was varied by small increments at the crossover into the $3d$ scaling region. Throughout this work we used a large lattice temporal extent $L_t = 12$ in order to minimize discretization effects.

First, we present the results for the $(3 + 1)d$ Ising model. For certain values of κ we monitored finite size effects on the order parameter by simulating the model on lattices with two different values of spatial extent L_s . For the final analysis we chose the data sets for which the systematic errors on Σ are less than 0.5%. More precisely for the range of couplings $0.15040 \leq \kappa \leq 0.15100$ we chose $L_s = 48$, for $0.15010 \leq \kappa \leq 0.15030$ $L_s = 72$ and for $0.14993 \leq \kappa \leq 0.150075$ $L_s = 96$. For each value of κ we typically generated 10^6 sweeps of the algorithm. The magnetization data was fitted to the form

$$\Sigma = A(\kappa - \kappa_c)^{\beta_{\text{mag}}}. \quad (4.1)$$

The results for different ranges of κ are presented in Table 1. The simple power law fit is very good for data close to the transition, i.e. for $\kappa \leq 0.15005$. For these fits the exponent β_{mag} is consistent within error with a recent estimate of the critical index of the $3d$ Ising model $\beta_{\text{mag}}^{3d} = 0.3269(6)$ [14]. As shown in Table 1, the value of β_{mag} deviates from the $3d$ values and the quality of the fit gets worse as we include more data points at larger values of κ . Therefore, we conclude that the crossover to the $3d$ universality class occurs at $\kappa_{\text{cross}} \approx 0.150075$. The data and the fitting curve to the data with $\kappa \leq 0.150025$ are shown in Fig. 1. The statistical errors are smaller than the size of the symbols and for this reason we don't plot them in the figure. The data for the susceptibility and the correlation length for these values of the coupling were very noisy and did not allow us to measure the exponents γ and ν .

range of κ	β_{mag}	κ_c	$\chi^2/\text{d.o.f.}$
0.14993 - 0.150025	0.32(3)	0.149867(9)	0.3
0.14993 - 0.15005	0.34(2)	0.149863(7)	0.5
0.14993 - 0.150075	0.37(1)	0.149870(5)	1.1
0.14993 - 0.150100	0.37(1)	0.149853(5)	7.3

Table 1: Values of β_{mag} for the $(3 + 1)d$ Ising model extracted from different ranges of κ .

We measured the values of the spatial and temporal correlation lengths at the crossover into the $3d$ Ising scaling region by performing a simulation at $\kappa = 0.150075$ on a 12×48^3

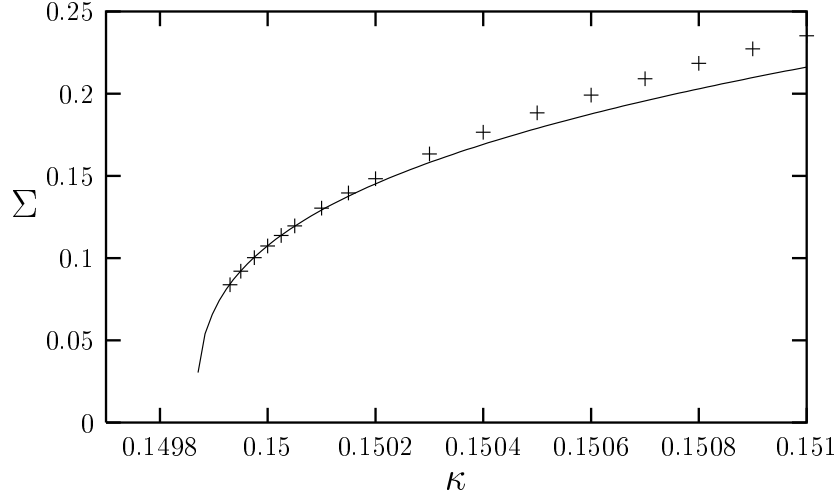


Figure 1: Order parameter vs. coupling for the $(3+1)d$ Ising model. The curve represents the fit to the data for $\kappa \leq 0.15005$.

lattice. For this measurement we chose a lattice with smaller spatial size L_s , because the correlation function was very noisy and we had to generate 15 million configurations in order to measure the correlation lengths ξ^t and ξ^s with statistical errors less than 7%. By fitting the temporal and spatial correlation functions to the single-pole ansatz we extracted $\xi^t = 6.5(4)$ and $\xi^s = 8.8(5)$. The overall error was estimated from the observation of the fit sensitivity to the variation of the parameters and to the range of points used in the fit. We conclude that in order to enter the $3d$ scaling region it was not necessary to work so close to the transition itself that the correlation lengths would be large compared to the temporal extent of the lattice. The importance of this comment lies in the fact that the formal derivations of the dimensional reduction scenario require that the zero mode dominates the Matsubara sum and this occurs when the scalar mass is small compared to the temperature. Apparently, our result shows that the higher Matsubara frequencies do not affect the critical singularities but they do affect non-universal aspects of the transition such as the width of the scaling region.

As the temperature approaches T_c the mass of the sigma meson decreases to zero and this results in an increase of the mesonic number density. A consequence of this is that the spectral function may become broader due to collisional broadening. One can study in detail the properties of the mesons at $T \neq 0$ by using the maximum entropy method to extract their spectral functions from high statistics correlation functions measured on anisotropic lattices with temporal sizes larger than $L_t = 12$. However, for our purposes the $L_t = 12$ temporal extent is large enough for an estimate of ξ^t at κ_{cross} . To the extent that we recognized particle-like excitations at $T \neq 0$ and $\xi^t \neq \xi^s$, implies that at κ_{cross} the

breaking of Lorentz invariance caused a significant “renormalization” of the speed of light in the mesonic dispersion relation.

range of κ	L_s	β_{mag}	κ_c	$\chi^2/\text{d.o.f}$
0.3125 - 0.3275	24	0.340(1)	0.30358(7)	0.5
0.3125 - 0.3275	48	0.343(2)	0.30362(1)	1.1
0.3125 - 0.3325	48	0.335(1)	0.30390(6)	5.6
0.3125 - 0.3375	48	0.329(1)	0.30417(4)	7.8

Table 2: Values of β_{mag} for the $(3+1)d$ $O(2)$ model extracted from different ranges of κ .

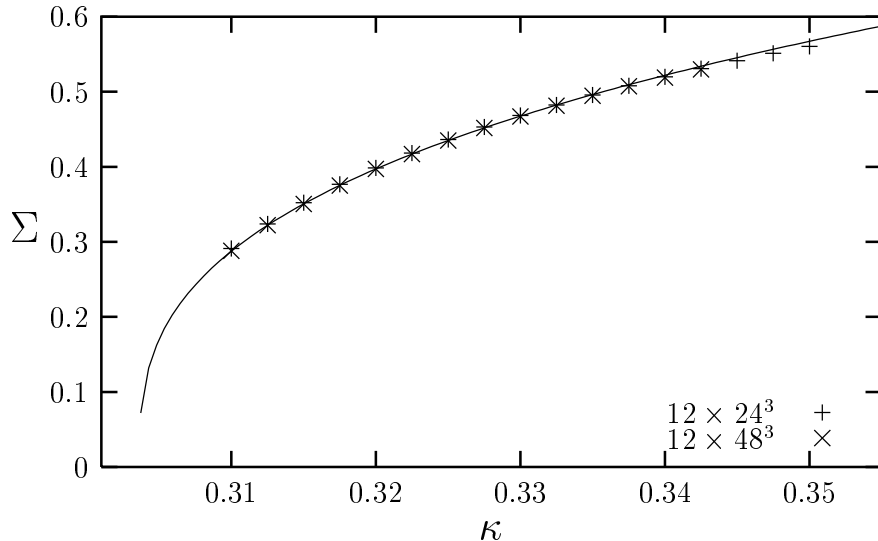


Figure 2: Order parameter vs. coupling for the $(3+1)d$ $O(2)$ model measured on 12×24^3 and 12×48^3 lattices. The curve represents the power law fit to the data for $\kappa \leq 0.3275$.

In this paragraph we discuss the numerical results in the low temperature phase of the $O(2)$ symmetric sigma model. We generated approximately 80,000 configurations for each value of the coupling on the 12×24^3 lattice and approximately 40,000 configurations for each value of κ on the 12×48^3 lattice. The results for the fits of Σ to the standard scaling law for different values of κ are shown in Table 2. By monitoring the change in the quality of the fits and the deviation in the value of β_{mag} from recent estimates of $\beta_{\text{mag}}^{3d} = 0.3485(2)$ [15] we conclude that $\kappa_{\text{cross}} \approx 0.3325$. An interesting observation is that finite size effects are negligible even when the asymmetry ratio is two. In Fig. 2 we plot the order parameter versus coupling. The continuous line represents the power law fit to the 12×48^3 data for $\kappa \leq 0.3275$.

The values of the spatial and temporal correlation lengths measured at the crossover coupling $\kappa_{\text{cross}} = 0.3325$ are $\xi_{\text{cross}}^s = 0.94(2)$ and $\xi_{\text{cross}}^t = 0.97(3)$. We conclude that in the

$O(2)$ model the crossover to the $3d$ universality class occurs at a much smaller value of ξ/L_t than in the $O(1)$ model. This explains why the critical region in this case is more easily accessible on lattices with a smaller asymmetry ratio than in the case of the Ising model. The fact that the value of ξ_{cross}^t is very close to the value of ξ_{cross}^s implies that the thermal fluctuations are relatively small at the crossover into the $3d$ scaling region. The diverging correlation length of the Goldstone boson is a source of additional finite size effects in a system. In this case however, the values of the order parameter in the $3d$ scaling region measured on small lattices are close to its thermodynamic limit values, because the Goldstone boson had the effect of increasing the width of the critical region.

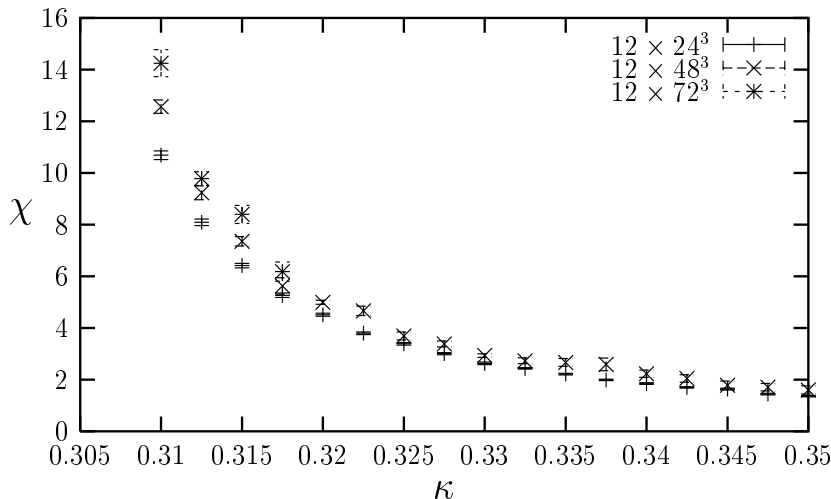


Figure 3: Susceptibility vs. coupling for the $(3+1)d$ $O(2)$ model measured on 12×24^3 , 12×48^3 and 12×72^3 lattices.

In Fig. 3 we present the results for the susceptibility χ of the order parameter for the $O(2)$ model. As expected finite size effects and statistical errors are much bigger for χ than for Σ and for this reason we are unable to extract a meaningful value for the exponent γ .

range of κ	L_s	β_{mag}	κ_c	$\chi^2/\text{d.o.f}$
0.4725 - 0.4875	48	0.377(4)	0.4569(2)	2.5
0.4725 - 0.4875	72	0.364(4)	0.4574(2)	0.4
0.4725 - 0.4975	72	0.356(2)	0.4579(1)	3.5
0.4725 - 0.4500	72	0.351(1)	0.4580(1)	4.0

Table 3: Values of β_{mag} for the $(3+1)d$ $O(3)$ model extracted from different ranges of κ .

We also performed simulations of the $O(3)$ model on lattices with sizes 12×48^3 and 12×72^3 and we observed a similar scenario to the one described above for the $O(2)$ model. Again, we generated approximately 30,000 to 50,000 configurations for each value of κ

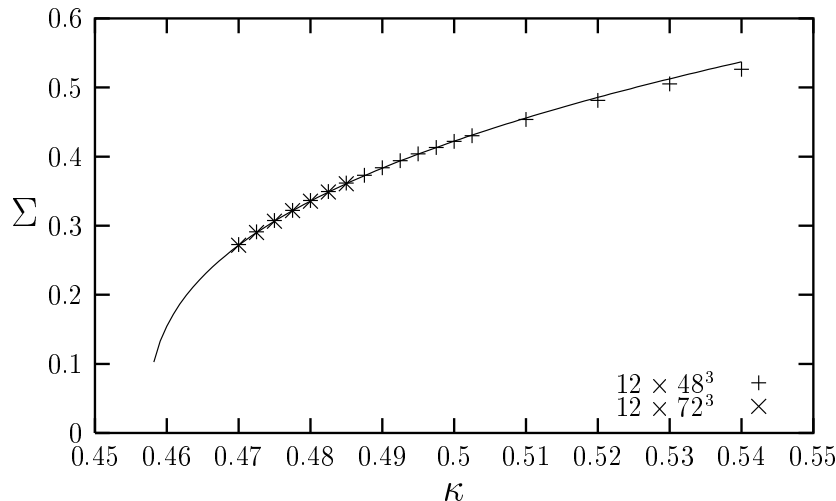


Figure 4: Order parameter vs. coupling for the $(3+1)d$ $O(3)$ model measured on 12×48^3 and 12×72^3 lattices. The curve represents the power law fit to the data for $\kappa \leq 0.4875$.

on both lattice sizes. The values of β_{mag} extracted from fits near the transition are very close to recent numerical results which predicted $\beta_{\text{mag}}^{3d} = 0.3689(3)$ [16]. The discrepancy in the values of β_{mag} extracted from the simulations on the two different lattice sizes and the difference in the value of $\chi^2/\text{d.o.f.}$ could be attributed to finite size effects on the smaller lattice. As expected the finite size effects in the $O(3)$ model are larger than in the $O(2)$ model, because it has twice as many Goldstone bosons. Again by monitoring the quality of the fit and the deviation of β_{mag} from β_{mag}^{3d} we found that the crossover into the $3d$ scaling region occurs at $\kappa_{\text{cross}} \approx 0.4975$. The values of the spatial and temporal correlation lengths measured on a 12×24^3 lattice at the crossover coupling $\kappa_{\text{cross}} = 0.4975$ are $\xi_{\text{cross}}^s = 0.92(3)$ and $\xi_{\text{cross}}^t = 0.90(2)$. Given the uncertainty in the measurement of the κ_{cross} , we conclude that the crossover in the $O(2)$ and $O(3)$ models occurs at approximately the same value of the correlation length.

range of κ	L_s	statistics
0.22425 - 0.22800	240	100,000
0.22404 - 0.22417	480	300,000
0.22400, 0.22404	720	500,000

Table 4: Lattice sizes and statistics at different values of κ for the $(2+1)d$ Ising model simulations.

We also performed simulations of the $(2+1)d$ Ising model. The results for the order parameter are shown in Fig. 5. In this case, because the dimensionality is lower, the infrared fluctuations are stronger than in the $(3+1)d$ model with the same symmetry. Therefore, in order to suppress finite size effects we simulated the model on lattices with larger asymmetry

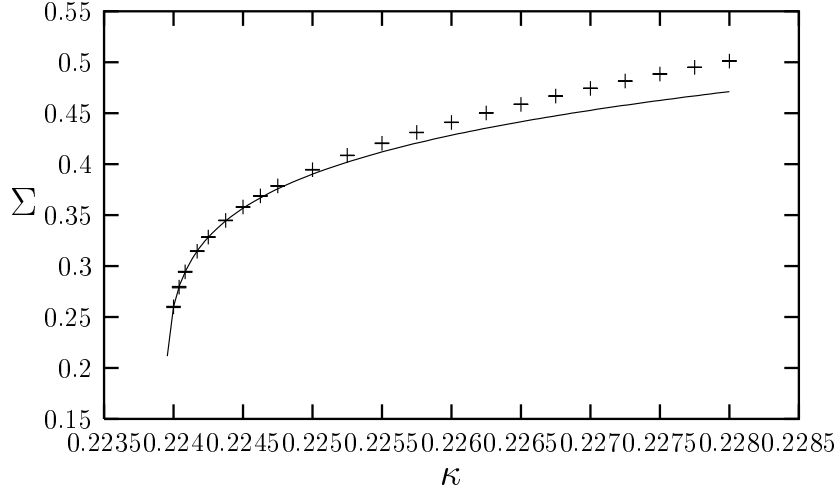


Figure 5: Order parameter vs. coupling for $(2+1)d$ Ising model. The curve represents the power law fit to the data for $\kappa \leq 0.2240$.

ratios than in the $(3+1)d$ case. The values of L_s and the amount of statistics generated at various values of κ are shown in Table 4. By fitting the data with the four smallest values of κ to the standard scaling relation we extracted $\kappa_c = 0.22394(1)$ and $\beta_{\text{mag}} = 0.138(8)$, which is close to the $2d$ Ising exponent $\beta_{\text{mag}}^{2d} = 0.125$. We conclude that the crossover into the $2d$ scaling region is at $\kappa_{\text{cross}} \approx 0.22417$. The value of the spatial correlation length at κ_{cross} measured on a 12×240^2 lattice by generating 5.5 million configurations is $\xi_{\text{cross}}^s = 25.0(2.0)$. Unfortunately, the large statistical fluctuations in the data set did not allow us to measure the temporal correlation length.

Next, we present results in the symmetric phase of the $O(2)$ model. We measured the improved estimators for the susceptibility (see eq. (3.5)), for the exponential correlation length ξ_{exp} extracted from the asymptotic decay of $C(t)_{\text{imp}}$ (see eq. (3.8)) and for the second moment correlation length $\xi_{2\text{nd}}$ (see eq. (3.10)). It is well-known that in the high temperature phase of this model $L_s/\xi \approx 7$ is sufficient to give thermodynamic limit results. In order to detect finite size effects, we performed simulations at $\kappa = 0.2930$ on lattices with $L_s = 24$ and 36 and we found that in both cases the values of the susceptibility and the correlation lengths agree within errors, implying that finite-size effects are under control. In most cases we kept $L_s/\xi > 9$ by increasing L_s from 24 to 96 as we approached the critical coupling with constant $L_t = 12$. For each value of the coupling we generated approximately 10^7 configurations. We also checked that the deviations between ξ_{exp} and $\xi_{2\text{nd}}$ are less than 0.5% for all the values of κ . An interesting observation is that ξ^t and ξ^s remain equal for all values of κ studied in this work. The value of κ which is closest to κ_c is 0.3015 and $\xi = 14.18(7)$ at this value of the coupling. This observation implies that in the symmetric phase the

quantum fluctuations remain more important than the thermal fluctuations up to relatively large values of ξ/L_t .

range of κ	range of ξ^s	γ	ν
0.2800 - 0.2970	1.691(2) - 4.003(7)	1.11(1)	0.602(4)
0.2990 - 0.3015	5.33(3) - 14.18(7)	1.18(1)	0.59(1)

Table 5: Values of γ and ν measured in the symmetric phase of the $(3+1)d$ $O(2)$ model in different ranges of κ and ξ^s .

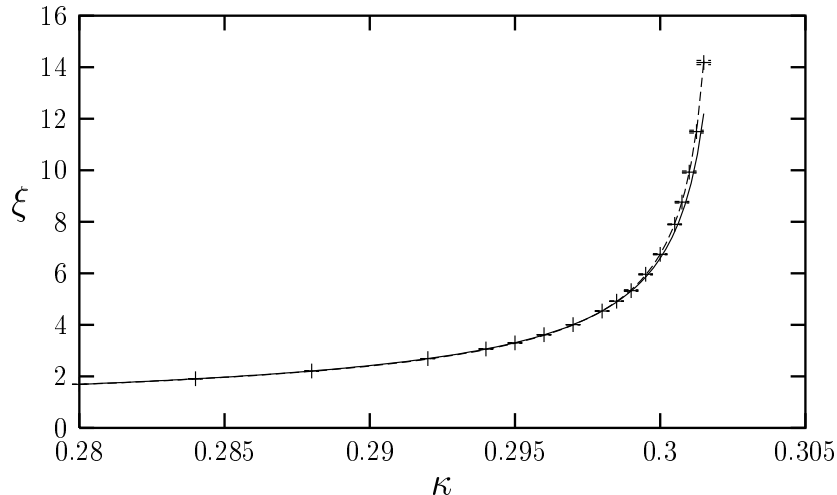


Figure 6: Correlation length vs. coupling measured in the symmetric phase of the $(3+1)d$ $O(2)$ model. The continuous line represents the fit to the data for $0.2800 \leq \kappa \leq 0.2970$ and the dashed line represents the fit for $0.2990 \leq \kappa \leq 0.3015$.

We also measured the exponents γ and ν in the $O(2)$ -symmetric phase by fitting our data to the standard scaling laws

$$\chi = B(\kappa_c - \kappa)^{-\nu}; \quad \xi = C(\kappa_c - \kappa)^{-\gamma}. \quad (4.2)$$

The results for the fits in different scaling windows are shown in Table 5. The data and the fitting curves are shown in Figs. 6 and 7. The exponents measured are significantly different from recent predictions of the three-dimensional critical exponents $\gamma^{3d} = 1.3177(5)$ and $\nu^{3d} = 0.67155(27)$ [15]. Our results are consistent however, with the observation mentioned above that in the symmetric phase the thermal fluctuations do not influence decisively the critical properties of the model even up to values of the correlation length that are much larger than the value of ξ_{cross} in the broken phase.

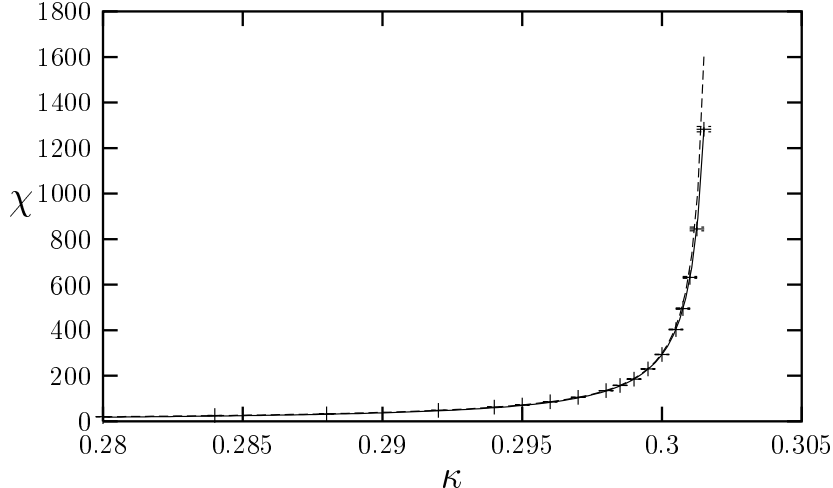


Figure 7: Susceptibility vs. coupling measured in the symmetric phase of the $(3 + 1)d$ $O(2)$ model. The continuous line represents the fit to the data for $0.2800 \leq \kappa \leq 0.2970$ and the dashed line represents the fit for $0.2990 \leq \kappa \leq 0.3015$.

5. Conclusions

We presented results from numerical simulations of the $O(N)$ sigma model at finite temperature for $N = 1, 2, 3$ in four dimensions and $N = 1$ in three dimensions. We investigated the phenomenon of dimensional reduction and studied the dependence of the width of the critical region on the number of field components N and on whether the $O(N)$ symmetry is spontaneously broken or restored. Contrary to the naive geometric scenario which requires that the condition $\xi \gg L_t$ must be satisfied in order to reach the $d - 1$ scaling region, we showed that in the low temperature phase the correlation length of the sigma meson doesn't have to be much larger than L_t in order to reach the dimensionally reduced critical region. Our results imply that the nonzero Matsubara modes do not affect the critical singularities but they can affect non-universal aspects of the transition such as the width of the scaling region. We measured the correlation length of the sigma meson in the temporal and spatial directions at the crossover into the $d - 1$ scaling region and we found that for $\frac{\Lambda}{T} = L_t = 12$ in the case of the $O(2)$ model $\xi_{\text{cross}}^t = 0.94(2)$ and $\xi_{\text{cross}}^s = 0.97(3)$ and for the $O(3)$ model $\xi_{\text{cross}}^t = 0.90(2)$ and $\xi_{\text{cross}}^s = 0.92(3)$. We should note however, that the deviations from the $3d$ scaling laws at these relatively small correlation lengths should also be affected by discretization effects. In the case of the Ising model we measured $\xi_{\text{cross}}^t = 6.5(4)$ and $\xi_{\text{cross}}^s = 8.8(5)$, implying that the critical region is much wider in the presence of the infrared fluctuations due to the Goldstone bosons. The critical regions for $N = 2$ and 3 have approximately the same width and therefore we don't expect a significant change in the width of the scaling

region for $N > 3$. The fact that for the continuous symmetries $\xi_{\text{cross}}^s \approx \xi_{\text{cross}}^t$ implies that the thermal fluctuations are still very small at the crossover temperature.

It is not yet known whether the dimensional reduction scenario is the correct description of the QCD thermal phase transition. If it is, then the thermal transition with massless quarks may belong to the $O(4)$ universality class, whereas when the quarks are massive the tricritical point in the (μ, T) plane becomes critical and it must belong to the $3d$ Ising universality class. According to our results the latter must have a much thinner scaling region than the massless quarks transition.

We also showed that the critical region of the $(3 + 1)d$ $O(2)$ model in the symmetric phase is much thinner than in the broken phase. Despite the fact that we simulated the model very close to the critical point and went up to correlation lengths ≈ 14 , the values of the measured exponents are not consistent with the $3d$ exponents; they are rather effective exponents with values between mean field exponents and $3d$ exponents.

We also studied the symmetry restoration transition in the $(2 + 1)d$ Ising model. This model has a well-defined interacting continuum limit and its behavior near T_c is particularly hard to explore analytically, because infrared divergences get worsened in three dimensions. We showed that in order to reach the $2d$ scaling region on lattices with temporal extent $L_t = 12$ the spatial correlation length $\xi^s = 25.0(2.0)$ and in order to minimize finite size effects the simulations near T_c were performed on lattices with large spatial extents that are larger by almost an order of magnitude than in the four-dimensional case. In this lower dimensionality we studied only $N = 1$, because according to the Coleman-Mermin-Wagner theorem [17] for any continuous symmetry in two spatial dimensions the infrared divergent fluctuations wash out the order parameter and the symmetry is manifest for $T > 0$.

In the future we would like to study the width of the scaling region of the $O(N)$ linear sigma model and compare with the results from the nonlinear sigma model presented in this paper. It was shown in the past that the dimensional reduction scenario is the correct description of the chiral phase transition in four-fermion models [18], because the infrared region is dominated by the zero Matsubara mode of the bosonic field and the nonzero bosonic and fermionic modes decouple. Simulations of the $(3 + 1)d$ four-fermion model with Z_2 and $SU(2) \times SU(2)$ chiral symmetries are underway in order to study the dependence of the width of the critical region on the degree of chiral symmetry of the model.

Acknowledgments

Discussions with Simon Hands and John Kogut are greatly appreciated. Costas Strouthos was supported by a Leverhulme Trust grant. Ioannis Tziligakis was partially supported by the Research Board at the University of Illinois, RES BRD KOGUT J 1-1-28212. Funds provided by this grant were used to purchase a dual processor Pentium IV, 2.2 Ghz computer, on which the simulations were carried out. Ioannis Tziligakis would also like to thank Costas Papanikolas and the Institute for Accelerator Systems and Applications (IASA) at the University of Athens, Greece for their hospitality in the fall of 2002.

References

- [1] D.A. Kirzhnits and A.D. Linde, Phys. Lett. **B42**, 471, (1972); S. Weinberg, Phys. Rev. **D9**, 3357 (1974); L. Dolan and R. Jackiw, Phys. Rev. **D9**, 3320 (1974).
- [2] D. O'Connor and C.R. Stephens, Nucl. Phys. **B360**, 297 (1991); *ibid.* Mod. Phys. Lett. **A8**, 1770 (1993); *ibid.* Phys. Rev. Lett. **72**, 506 (1994); O. Bohr, D.-J. Schaefer and J. Wambach, Int. J. Mod. Phys. **A16**, 3823 (2001); S.-B. Liao and M. Strickland, Nucl. Phys. **B497**, 611 (1997); *ibid.* Strickland, Nucl. Phys. **B532**, 753 (1998); N. Tetradis and C. Wetterich, Nucl. Phys. **B398**, 659 (1993); *ibid.*, Nucl. Phys. **B401**, 567 (1993).
- [3] F. Wilczek, Int. J. Mod. Phys. **A7**, 3911 (1992); R.D. Pisarski and F. Wilczek, Phys. Rev. **D29**, 338 (1984).
- [4] M.A. Stephanov, Phys. Rev. **D52**, 3746 (1995).
- [5] K. Jansen and P. Seufferling, Nucl. Phys. **B343**, 507 (1990).
- [6] W.A. Bardeen and M. Moshe, Phys. Rev. **D28**, 1372 (1983).
- [7] I. Ya Aref'eva, E.R. Nissimov and S.J. Pacheva, Commun. Math. Phys. **71**, 213 (1980).
- [8] G. Bimonte, D. Iniguez, A. Tarancon and C.L. Ullod, Nucl. Phys. **B 490**, 701 (1997).
- [9] U. Wolff, Phys. Rev. Lett. **62**, 361 (1989).
- [10] A. Hasenfratz, K. Jansen, J. Jersak, C.B. Lang, T. Neuhaus and H. Yoneyama, Nucl. Phys. **317**, 81 (1989).
- [11] A. Hasenfratz, K. Jansen, J. Jersak, C.B. Lang, H. Leutwyler and T. Neuhaus, Z. Phys. **C46**, 257 (1990).
- [12] M. Hasenbusch, Nucl. Phys. **B333**, 507 (1990).

- [13] M. Caselle and M. Hasenbusch, *J. Phys.* **A30**, 4963 (1997).
- [14] A.L. Talapov and H.W.J. Blote, *J. Phys.* **A 29**, 5727 (1996).
- [15] M. Campostrini, M. Hasenbusch, A. Pelissetto, P. Rossi and E. Vicari, *Phys. Rev.* **B63**, 214503 (2001).
- [16] M. Campostrini, M. Hasenbusch, A. Pelissetto, P. Rossi and E. Vicari, *Phys. Rev.* **B65**, 144520 (2002).
- [17] S. Coleman, *Commun. Math Phys.* **31**, 259 (1961); N.D. Mermin and H. Wagner, *Phys. Rev. Lett.* **17**, 1133 (1966).
- [18] J.B. Kogut, M.A. Stephanov and C.G. Strouthos, *Phys. Rev.* **D58**:096001 (1998); S. Chandrasekharan, J. Cox, K. Holland and U.J. Wiese, *Nucl. Phys.* **B576**, 481 (2000).